J Electr Eng Technol Vol. 7, No. 6: 905-910, 2012
http://dx.doi.org/10.5370/JEET.2012.7.6.905

ISSN(Print) 1975-0102
ISSN(Online) 2093-7423

Thermal Analysis of Interior Permanent-Magnet Synchronous Motor by Electromagnetic Field-Thermal Linked Analysis

Sang-Taek Lee*,, Hee-Jun Kim*, Ju-hee Cho**, Daesuk Joo† and Dae-kyong Kim*****

Abstract – This paper reports an investigation of pulse width modulation (PWM) techniques for two-phase brushless DC (BLDC) motors fed by a two-phase eight-switch inverter in a fan application. The three-phase BLDC motor is widely applied in industry; however, a lower-cost two-phase BLDC motor and drive circuit has been greatly in demand in recent years. In this paper, we introduce a mathematical model of the two-phase BLDC motor with sinusoidal back electromotive forces (EMFs) based on traditional three-phase BLDC motors. To simplify the drive algorithm and speed up its application, we analyze the principle of block commutation for a two-phase BLDC motor drive in the 180-electrical-degree conduction mode, and we further propose five PWM schemes to improve the commutation performance of the two-phase BLDC drive. The effectiveness of the proposed PWM methods is verified through experiments.

Keywords: Thermal analysis, Analytical models, Numerical models, Permanent-magnet motors

1. Introduction

The electric farm tractors, traction engines, used electric motor for power. The use of these tractors, instead of diesel-powered tractors, provides quieter, eco-friendly transportation that does not pollute the air. Interior permanent-magnet synchronous motors (IPMSMs) for electrically powered tractors offer a variety of advantages, including high efficiency and high motor power density. Limits to the operating time of IPMSMs are set by the allowed maximum operating temperature for insulation and/or permanent-magnet materials. Thermal analysis is therefore important in the predicting temperature of IPMSMs and there are the most used techniques: lumped-parameter (LP) thermal analysis and finite-element method (FEM) thermal analysis. The most recent review dealt with an extended survey on the evolution and the modern approaches in the thermal analysis of electrical machines [1]. The journal literatures on thermal analysis of electric motors are [2-7], describing induction motors; [8-13], dealing with permanent-magnet motors. The thermal analysis of IPMSMs has received less attention than other machines. [5, 9, 14] show the coupled electromagnetic-thermal analysis of some electrical machines. However, the analysis of IPMSM by combined electromagnetic-thermal model has received less attention than other machines.

This paper presents the results of thermal analysis and shows a comparison between the measurements of temperature and our predictions. To predict a prototype IPMSM temperature, we linked the results of electro-magnetic field analysis with both LP thermal analysis and 3-D FEM thermal analysis. The motor used in the electric tractor is IPMSM without cooling system (7.5 kW, class F insulation system) shown in Fig. 1.

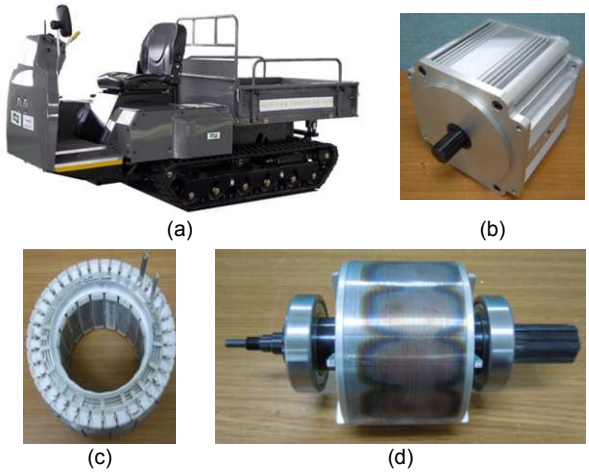

Fig. 1. (a) Developed smaller electric tractor: (b) prototype IPMSM; (c) stator; (d) interior permanent-magnet rotor.

2. Lumped-Parameter Thermal Analysis

2.1 Lumped-parameter thermal model

The structure of an IPMSM can be subdivided into the

† Corresponding author: Dept. of Electrical Engineering, Pukyong National University, Korea. (201156066@pknu.ac.kr)
* Dept. of Electronics, Electrical, Control and Instrumentation Engineering, Hanyang University, Korea. (stlee@hanyang.ac.kr, hjkim@hanyang.ac.kr)
** Korea Electronics Technology Institute, Korea. (jhcho@keti.re.kr)
*** Dept. of Electrical Control Engineering, Sunchon National University, Korea. (dkkim@sunchon.ac.kr)
Received: November 4, 2011; Accepted: August 20, 2012

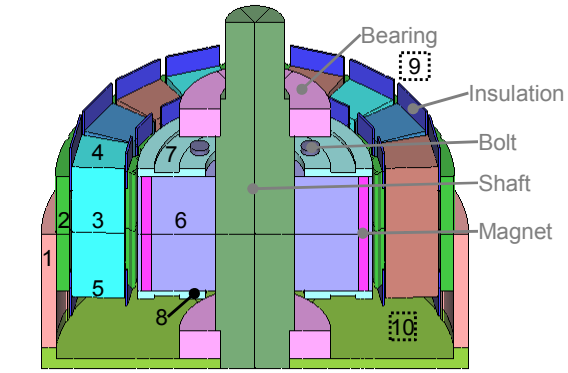

1. Frame, 2. Stator, 3. Winding, 4.,5. End winding
6. Rotor, 7.,8. Magnet support, 9.,10. Inner air

Fig. 2. Prototype IPMSM structure.

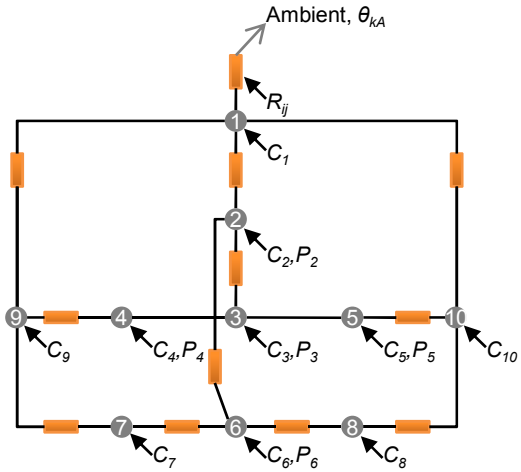

Fig. 3. Simple lumped-parameter thermal model.

10 components shown in Fig. 2. To analytically calculate the temperature, we modeled LP thermal model for heat-transfer shown in Fig. 3. The thermal model is very simple to include the major components such as winding, stator, and rotor. The analytical model is well-known. In the LP thermal model, the rotor core and the permanent-magnet consolidated for easier calculation. Furthermore, all the thermal parameters (e.g., electric conductivity, thermal conductivity, specific heat, etc) are assumed to be constant.

In addition, any heat transfer due to radiation is neglected. All interference gaps between components set 0.1 mm except for interface gap between the winding and the stator. Initial temperature was set to 25°C. Typical value of the heat transfer coefficient for free convection is in the range 2 to 25 W/ (m^2·°C) [15]. In this model, the free convection heat transfer coefficient was set to 10 W/ (m^2·°C). In the thermal model, heat source is the average losses obtained by electromagnetic field analysis at rated operation. According to [1] and [2], the thermal resistance and the thermal capacitance for the machine are given in Table 1.

Table 1. Computed Lumped-Parameters

Thermal Resistance	VALUE [°C/W]	Thermal capacitance	Value [J/(kg·°C)]	Average Loss	Value [W]
R_{1A}	0.545	C_1	5650.0	P2	179.3
R_{12}	0.084	C_2	3044.3	P3	74.1
R_{19}	1.262	C_3	502.9	P4	11.7
R_{110}	1.262	C_4	78.7	P5	11.7
R_{23}	0.048	C_5	78.7	P6	48
R_{26}	0.176	C_6	2012.9		
R_{49}	1.016	C_7	88.7		
R_{510}	1.016	C_8	88.7		
R_{67}	0.412	C_9	7.5		
R_{68}	0.412	C_{10}	7.5		
R_{79}	11.111				
R_{810}	11.111				

2.2 Thermal network equations

The LP thermal model consists of 10 nodes. The individual node network equations are

$$P_1 = C_1\frac{d\theta_1}{dt} + \frac{1}{R_{1A}}(\theta_1-\theta_{kA}) + \frac{1}{R_{12}}(\theta_1-\theta_2) + \frac{1}{R_{19}}(\theta_1-\theta_9) + \frac{1}{R_{110}}(\theta_1-\theta_{10}) \quad (1a)$$

$$P_2 = C_2\frac{d\theta_2}{dt} + \frac{1}{R_{12}}(\theta_2-\theta_1) + \frac{1}{R_{23}}(\theta_2-\theta_3) + \frac{1}{R_{26}}(\theta_2-\theta_6) \quad (1b)$$

$$P_3 = C_3\frac{d\theta_3}{dt} + \frac{1}{R_{23}}(\theta_3-\theta_2) \quad (1c)$$

$$P_4 = C_4\frac{d\theta_4}{dt} + \frac{1}{R_{49}}(\theta_4-\theta_9) \quad (1d)$$

$$P_5 = C_5\frac{d\theta_5}{dt} + \frac{1}{R_{510}}(\theta_5-\theta_{10}) \quad (1f)$$

$$P_6 = C_6\frac{d\theta_6}{dt} + \frac{1}{R_{26}}(\theta_6-\theta_2) + \frac{1}{R_{67}}(\theta_6-\theta_7) + \frac{1}{R_{68}}(\theta_6-\theta_8) \quad (1g)$$

$$P_7 = C_7\frac{d\theta_7}{dt} + \frac{1}{R_{67}}(\theta_7-\theta_6) + \frac{1}{R_{79}}(\theta_7-\theta_9) \quad (1h)$$

$$P_8 = C_8\frac{d\theta_8}{dt} + \frac{1}{R_{68}}(\theta_8-\theta_6) + \frac{1}{R_{810}}(\theta_8-\theta_{10}) \quad (1i)$$

$$P_9 = C_9\frac{d\theta_9}{dt} + \frac{1}{R_{19}}(\theta_9-\theta_1) + \frac{1}{R_{49}}(\theta_9-\theta_4) + \frac{1}{R_{79}}(\theta_9-\theta_7) \quad (1j)$$

$$P_{10} = C_{10}\frac{d\theta_{10}}{dt} + \frac{1}{R_{110}}(\theta_{10} - \theta_1) + \frac{1}{R_{510}}(\theta_{10} - \theta_5) + \frac{1}{R_{810}}(\theta_{10} - \theta_8) \quad (1k)$$

$$\frac{d\theta_1}{dt} = \frac{P_1 + G_{1A}\theta_{kA}}{C_1} - \frac{1}{C_1}(G_{11}\theta_1 - G_{12}\theta_2 - G_{19}\theta_9 - G_{110}\theta_{10}), \quad (2a)$$
$$G_{11} = G_{1A} + G_{12} + G_{19} + G_{110}$$

$$\frac{d\theta_2}{dt} = \frac{P_2}{C_2} - \frac{1}{C_2}(G_{22}\theta_2 - G_{12}\theta_1 - G_{23}\theta_3 - G_{26}\theta_6), \quad (2b)$$
$$G_{22} = G_{12} + G_{23} + G_{26}$$

$$\frac{d\theta_3}{dt} = \frac{P_3}{C_3} - \frac{1}{C_3}(G_{33}\theta_3 - G_{23}\theta_2), G_{33} = G_{23} \quad (2c)$$

$$\frac{d\theta_4}{dt} = \frac{P_4}{C_4} - \frac{1}{C_4}(G_{44}\theta_4 - G_{49}\theta_9), G_{44} = G_{49} \quad (2d)$$

$$\frac{d\theta_5}{dt} = \frac{P_5}{C_5} - \frac{1}{C_5}(G_{55}\theta_5 - G_{510}\theta_{10}), G_{55} = G_{510} \quad (2e)$$

$$\frac{d\theta_6}{dt} = \frac{P_6}{C_6} - \frac{1}{C_6}(G_{66}\theta_6 - G_{26}\theta_2 - G_{67}\theta_7 - G_{68}\theta_8), \quad (2f)$$
$$G_{66} = G_{26} + G_{67} + G_{68}$$

$$\frac{d\theta_7}{dt} = \frac{P_7}{C_7} - \frac{1}{C_7}(G_{77}\theta_7 - G_{67}\theta_6 - G_{79}\theta_9), \quad (2g)$$
$$G_{77} = G_{67} + G_{79}$$

$$\frac{d\theta_8}{dt} = \frac{P_8}{C_8} - \frac{1}{C_8}(G_{88}\theta_8 - G_{68}\theta_6 - G_{810}\theta_{10}), \quad (2h)$$
$$G_{88} = G_{68} + G_{810}$$

$$\frac{d\theta_9}{dt} = \frac{P_9}{C_9} - \frac{1}{C_9}(G_{99}\theta_9 - G_{19}\theta_1 - G_{49}\theta_4 - G_{79}\theta_7), \quad (2i)$$
$$G_{99} = G_{19} + G_{49} + G_{79}$$

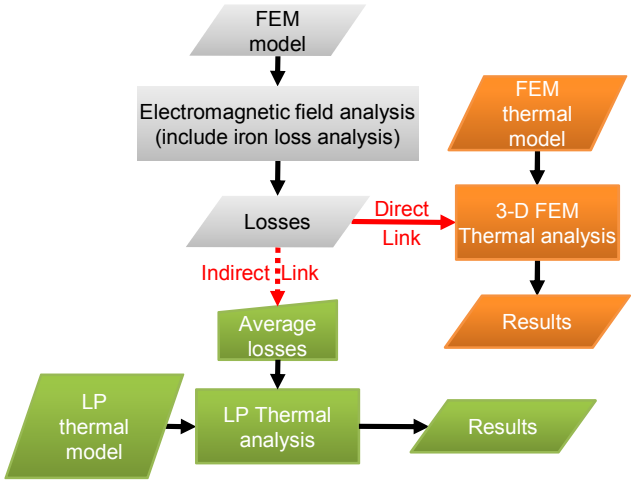

Fig. 4. Diagram of computation procedures.

$$\frac{d\theta_{10}}{dt} = \frac{P_{10}}{C_{10}} - \frac{1}{C_{10}}(G_{1010}\theta_{10} - G_{110}\theta_1 - G_{510}\theta_5 - G_{810}\theta_8), \quad (2j)$$
$$G_{1010} = G_{110} + G_{510} + G_{810}$$

where Pi is power loss at node i, Ci is node thermal capacitance, Rij is thermal resistance between adjoining nodes i and j, θi is node temperature, θkA is ambient temperature and is assumed to be constant. The differential equations are derived from (1), shown at the top of the next page. Where (2), Gij is thermal conductance. The differential equations are represented in matrix form by

$$\frac{d}{dt}[\theta] = [C]^{-1}[P] - [C]^{-1}[G][\theta] \quad (3)$$

where $[\theta]$ is a column matrix of temperatures, $[C]$ is a diagonal matrix of thermal capacitance, $[P]$ is a column matrix of power losses, $[G]$ is a square matrix of thermal conductance. Assuming that the temperatures are unchanging in time, the steady-state equation becomes

$$[\theta] = [G]^{-1}[P]. \quad (4)$$

3. Electromagnetic Field–Thermal Linked Analysis Using FEM

To numerically compute the temperature, we used FEM software package. The 3-D FEM model is sufficiently detailed to comprise all components shown in Fig. 2. The FEM thermal model has been computed in the same assumptions discussed in Section 2. Fig. 4 shows a diagram of computation procedures to calculate an IPMSM temperature by an electromagnetic field-thermal linked analysis. 3-D FEM thermal analysis results are linked with the LP thermal analysis.

4. Thermal Test, Results and Discussion

A prototype IPMSM thermal test has been performed at rated power (Fig. 5). Thermocouples were embedded in both the winding and the frame to measure the temperature of the prototype motor. At 50 minutes into the thermal test, the motor was turned off because the winding temperature was 156.3 °C. The rated operating time of the prototype motor should be limited to 50 minutes because allowed maximum operating temperature is below 155 °C.

Fig. 6 shows a comparison both thermal analyses at steady-state. The numerical prediction for the winding temperature shows a very similar behavior to the experimental temperature data (Fig. 7), but the accuracy of frame temperature is not so good. This is not too bad because the winding is a more critical component than

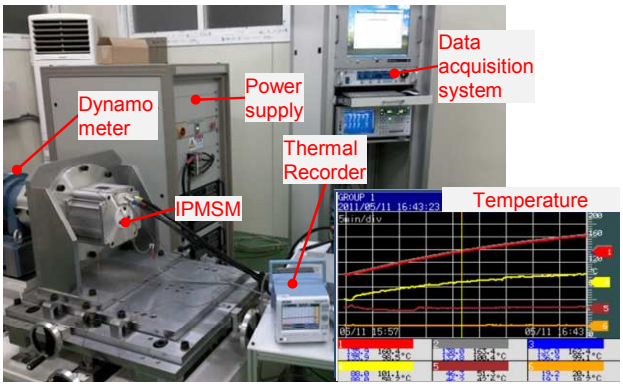

Fig. 5. Experimental set-up for a prototype IPMSM thermal test.

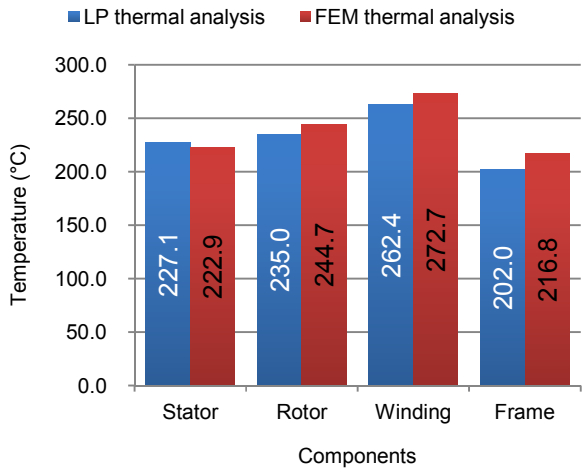

Fig. 6. Comparison both thermal analyses at steady-state.

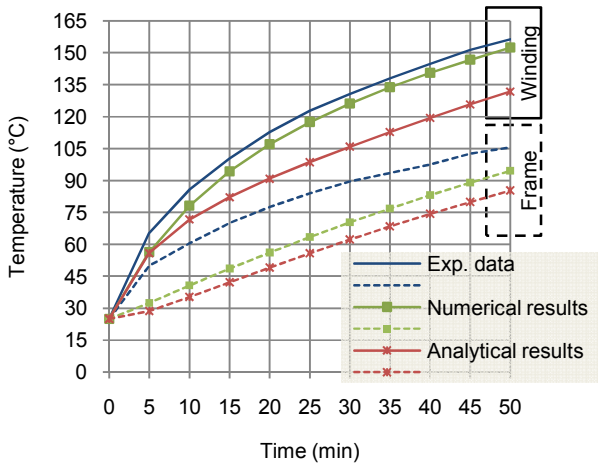

Fig. 7. Temperature predictions compared with experimental data.

frame. FEM thermal analysis seems more accurate than LP thermal analysis. Table 2 shows the predicted and measured temperatures at 50 minutes for the prototype motor.

Local temperature measurements such as using thermocouples give the machine operator confidence, but the temperature detectors may not be at the portion of rotor. Temperature measurements discussed so far have been on the portion of stator. However, the rotor is a critical component in many motors, particularly permanent-magnet motor under high temperature conditions. A high temperature will cause more demagnetization resulting in premature failure. As in the thermal analysis, the rotor temperature was near 100 °C at 50 minutes. The operating time of the prototype motor should be also limited to 50 minutes because the maximum operating temperature of neodymium permanent-magnet is 100 °C.

Table 2. Predicted and Measured Temperature at 50 minutes

Component	Predicted temperature [°C]		Measured temperature [°C]
	LP thermal analysis	FEM thermal analysis	
Winding	131.8	152.4	156.3
Frame	85.3	94.6	105.5
Stator	101.2	97.8	-
Rotor	101.8	97.4	-

5. Conclusion

A lumped-parameter thermal model of an IPMSM was modeled. The thermal model is very simple, but computed results show a similar value to the FEM results at steady-state. The analytical thermal model has the advantage of being very fast to compute temperature; however, there is still room for improvement in our thermal model. We anticipate that electromagnetic field-thermal linked analyses are able to predict the temperature variation of IPMSM. These thermal analyses are expected to help improve the thermal performance of prototype IPMSM.

Acknowledgements

This work was supported by the Energy Efficiency & Resources of the Korea Institute of Energy Technology Evaluation and Planning (KETEP) grant funded by the Korea government Ministry of Knowledge Economy. (No. 2010T100100797)

References

[1] A. Boglietti, A. Cavagnino, D. Staton, M. Shanel, M. Mueller, C. Mejuto, "Evolution and modern approaches for thermal analysis of electrical machines," *IEEE Trans. Industrial Electronics*, Vol. 56, No.3, pp. 871-882, Mar. 2009.

[2] P. H. Mellor, D. Roberts, D. R. Turner, "Lumped parameter thermal model for electrical machines of

TEFC design," *Electric Power Applications, IEE Proceedings B*, Vol.138, No.5, pp. 205-218, Sep. 1991.
[3] Yangsoo Lee, Song-Yop Hahn, S.K. Kauh, "Thermal analysis of induction motor with forced cooling channels," *IEEE Trans. Magnetics*, Vol. 36, No.4, pp. 1398-1402, July 2000.
[4] D. Staton, A. Boglietti, A. Cavagnino, "Solving the more difficult aspects of electric motor thermal analysis," *Electric Machines and Drives Conference, 2003. IEMDC'03. IEEE International*, Vol. 2, No., pp. 747-755, Vol. 2, 1-4 June 2003.
[5] S. Mezani, N. Takorabet, B. Laporte, "A combined electromagnetic and thermal analysis of induction motors," *IEEE Trans. Magnetics*, Vol. 41, No. 5, pp. 1572-1575, May 2005.
[6] O.I. Okoro, "Steady and transient states thermal analysis of a 7.5-kW squirrel-cage induction machine at rated-load operation," *IEEE Trans. Energy Conversion*, Vol. 20, No. 4, pp. 730-736, Dec. 2005.
[7] A. Boglietti, A. Cavagnino, M. Pastorelli, D. Station, A. Vagati, "Thermal analysis of induction and synchronous reluctance motors," *IEEE Trans. Industry Applications*, Vol. 42, No. 3, pp. 675-680, May-June 2006.
[8] YouGuang Guo, Jian Guo Zhu, W. Wu, "Thermal analysis of soft magnetic composite motors using a hybrid model with distributed heat sources," *IEEE Trans. Magnetics*, Vol. 41, No. 6, pp. 2124-2128, June 2005.
[9] D.G. Dorrell, "Combined thermal and electromagnetic analysis of permanent-magnet and induction machines to aid calculation," IEEE Trans. Industrial Electronics, Vol. 55, No. 10, pp. 3566-3574, Oct. 2008.
[10] F. Marignetti, V.D. Colli, "Thermal analysis of an axial flux permanent-magnet synchronous machine," IEEE Trans. Magnetics, Vol. 45, No. 7, pp. 2970-2975, July 2009.
[11] Yunkai Huang, Jianguo Zhu, Youguang Guo, "Thermal analysis of high-speed SMC motor based on thermal network and 3-D fea with rotational core loss included," *IEEE Trans. Magnetics*, Vol. 45, No. 10, pp. 4680-4683, Oct. 2009.
[12] S. Ruoho, J. Kolehmainen, J. Ikaheimo, A. Arkkio, "Interdependence of demagnetization, loading, and temperature rise in a permanent-magnet synchronous motor," *IEEE Trans. Magnetics,* Vol. 46, No. 3, pp. 949-953, Mar. 2010.
[13] Jinxin Fan, Chengning Zhang, Zhifu Wang, Yunang dong, C.E. Nino, A.R. Tariq, E.G. Strangas, "Thermal analysis of permanent magnet motor for the electric vehicle application considering driving duty cycle," *IEEE Trans. Magentics*, Vol. 46, No. 6, pp. 2493-2496, June 2010.
[14] P. K. Vong, D. Rodger, "Coupled electromagnetic-thermal modeling of electrical machines," *IEEE Trans. Magnetics*, Vol. 39, No. 3, pp. 1614-1617, May 2003.
[15] F. P. Incropera, D. P. DeWitt, T.L. Bergman, A. S. Lavine, *Fundamentals of Heat and Mass Transfer*, 6th ed., Hoboken, NJ:Wiley, 2006, pp. 6-8.

Sang-Taek Lee He received the B.S. degree in electrical engineering from the Seoul National University of Technology, Seoul, Korea, in 1999 and the M.S. degree in electrical engineering from Hanyang University, Seoul, in 2001. He is presently a Ph. D. candidate in the Department of Electronic, Electrical, Control and Instrumentation Engineering in Hanyang University, Korea. From 2003 to 2009, he was with the Digital Appliances Research Laboratory, Samsung Electronics, Suwon, Korea. He is currently a Researcher with the Digital Conversion Center, Korea Electronics Technology Institute, Gwangju, Korea. His current research interests are in electric machines and power electronics.

Hee-Jun Kim He received the B.S and M.S degrees in electronics engineering from Hanyang University, Seoul, Korea, in 1976 and 1978, respectively, and the Ph.D. degree in electronics engineering from Kyushu University, Fukuoka, Japan, in 1986. Since 1987, he has been with the School of Electrical Engineering and Computer Science, Hanyang University, Ansan, Korea, where he is currently a Professor. From 1991 to 1992, he was a Visiting Scholar with the Virginia Polytechnic Institute and State University, Blacksburg. His fields of interest include electric machine drives, Switching power converters, electronic ballasts, soft-switching techniques, and analog signal processing. Dr. Kim is the Vice President of Korea Institute of Electrical Engineers.

Ju-Hee Cho He received his B.S. degree in Electronics Engineering and M.S. degree in Department of Electronics, Control and Instrumentation Engineering from Hanyang University in 2001 and 2003, respectively. 2004, he was an engineer in the Central Research Institute, Hyundai Rotem. From 2005 to 2009, he worked for Komotek Co., as a Senior-Researcher. He is currently a Senior-Researcher at the Korea Electronics Technology Institute. His research interests are analysis and design of permanent magnet synchronous motor.

Daesuk Joo He received the B.S and M.S degrees in electrical engineering from the Pukyong National University, Busan, Korea, in 2008 and 2010, respectively. He is now a Ph.D. student in the Department of Electrical Engineering at the Pukyong National University. His research interests include electrical machines and coupled multi-physics problems. Since 2011, he has been a researcher at the Korea Electrotechnology Research Institute.

Dae-kyong Kim He received the M.S degrees in the Dept. of Electrical Engineering from Hanyang University, Korea, in 2001 and the Ph.D. degree in the Dept. of Electronics, Electrical, Control and Instrumentation Engineering in Hanyang University, Korea, in 2007, respectively. From 2001 to 2005, he was Senior Researcher with the Digital Appliances Research Laboratory, Samsung Electronics, Korea. From 2005 to 2011, he was Center Director with the Digital Convergence Research Center, Korea Electronics Technology Institute, Korea. He is currently Assistant Professor at sunchon National University. His research interests are design, numerical analysis and control of electrical machines.